

Quantum control of two interacting electrons in a coupled quantum dot

Ping Zhang^{1,2}, Xian-Geng Zhao²

¹*International Center of Quantum Structure and State Key laboratory for surface Physics, Institute of Physics, The Chinese Academy of Sciences, Beijing 100080, P.R. China*

²*Institute of Applied Physics and Computational Mathematics, Beijing 100080, P.R. China*

Quantum-state engineering, i.e., active manipulation over the coherent dynamics of suitable quantum-mechanical systems, has become a fascinating prospect of modern physics. Here we discuss the dynamics of two interacting electrons in a coupled quantum dot driven by external electric field. We show the two quantum dots can be used to prepare maximally entangled Bell state by varying the strength and duration of an oscillatory electric field. Different from suggestion given by Loss *et al.*[Phys. Rev. A, **57** (1998) 120], the present entanglement involves the spatial degree of freedom for the two electrons. We also find that the coherent tunneling suppression discussed by Grossmann *et al.*[Phys. Rev. Lett., **67** (1991) 516] persists in the two-particle case, i.e., two electrons initially localized in one dot can remain dynamically localized, although the strong Coulomb repulsion prevents them behaving so. Surprisingly, the interaction enhances the degree of localization to a larger extent compared to non-interacting case. We can call this phenomenon Coulomb-enhanced dynamical localization.

PACS numbers: 73.23.Hk, 73.61.-r, 78.66.-w, 78.7.+p

Keywords: coupled quantum dot, dynamical localization, entanglement

I. INTRODUCTION

Coherent control of quantum systems has been attracted considerable attentions in recent years. A basic ingredient of quantum control is field-induced localization of a single electron in a double-trap [1]. The initial efforts devoted to acquiring conditions to maintain existing localization with oscillatory electric field, and to create and maintain localization with a semi-infinite oscillatory field [2,3]. It was found that the investigation of localization can be approximated by a two-state model consisting of the lowest symmetric and antisymmetric states of the double-trap potential [4,5]. In this case, perfect localization can be achieved with a strong time-periodic electric field that causes the Floquet quasienergies to be degenerate. Later, localization in superlattice systems [6], in dissipative environments [7], in molecular systems [8], induced by ultrashort laser pulses, and in trapped Bose-Einstein condensates [9,10], by means of oscillatory magnetic fields, has been studied.

When two or more interacting particles are present, apart from the highly nontrivial problem of whether the strong many-body interaction can be overcome for the particles to create and preserve localization, the possibility of entanglement of the many-body wave functions

arises [11,12]. Entanglement is an essential ingredient in any scheme of quantum information processing like quantum information cryptography and quantum computation, and therefore it is a problem of great current interest to find or design systems where entanglement can be manipulated [13]. Most of the theoretical and experimental activity until now has been associated with atomic and quantum-optic systems. Two- [14,15], three- [16], and four-particle [17] entanglement have been successfully demonstrated experimentally in trapped ions, Rydberg atoms, and cavity QED. However, a further increase of the number of entangled particles in these systems is expected to be a severe experimental challenge. Recently, solid-state realizations of the entanglement have received increasingly attention due to the fact that semiconductor nanostructures such as quantum dots (QDs) and double quantum dots (DQDs) with well-defined atom-like and molecule-like properties, have been fabricated and studied by many groups [18,19]. Kane [20] has proposed a scheme which encodes information onto the nuclear spins of donor atoms in doped silicon electronic devices where externally applied electric fields are used to perform logical operations on individual spins. Loss and DiVincenzo [21] have presented a scheme based on spin exchange interaction effects. More recently, Imamoglu *et al.* [23] have considered a quantum computer model based on both electron spins and cavity QED which is capable of realizing controlled interactions between two distant quantum dots. Quiroga and Johnson [24] have suggested that the resonant transfer interaction between spatially separated excitons in quantum dots can be exploited to produce maximally entangled Bell states.

In the present work we study the coherent control of the quantum system consisting of two interacting electrons in a coupled quantum dot (see Fig. 1). With the initial state chosen to be in the spin-singlet space, the dynamics is reduced to be confined to a three-dimensional Hilbert space, in which the three basis vectors are equivalent to the eigenstates of \hat{z} component of spin-1 operator. We show that the maximally entangled Bell state can be prepared and maintained with a pulse of oscillatory electric field. Also we find that although the Coulomb repulsion between the two electrons is very strong, dynamical localization can fully build up in the system parameter manifold which corresponds to the exact crossing of the quasienergies developed from the unperturbed nearly-degenerate levels.

II. THE MODEL

The Hamiltonian which we use to describe the dynamics of two interacting electrons in a coupled quantum dot driven by electric fields is

$$H(t) = \sum_{i=1,2} h(\mathbf{r}_i, \mathbf{p}_i, t) + C, \quad (1a)$$

$$h(\mathbf{r}, \mathbf{p}, t) = \frac{\mathbf{p}^2}{2m} - ezF(t) + V_l(\mathbf{r}) + V_v(\mathbf{r}), \quad (1b)$$

$$C = \frac{e^2}{\kappa|\mathbf{r}_1 - \mathbf{r}_2|}, \quad (1c)$$

where C is the Coulomb interaction and h the single-particle Hamiltonian. The dielectric constant κ and the effective mass m are material parameters. The potential V_l in h describes the lateral confinement, whereas V_v models the vertical double-well structure. The lateral coupling of the dots is modeled by a quartic potential

$$V_l(x, y) = \frac{m\omega_z^2}{2} \alpha^2 (x^2 + y^2), \quad (2)$$

where we have introduced the isotropy parameter α determining the strength of the vertical relative to the lateral confinement. The lateral effective Bohr radius $a_{B\parallel} = \sqrt{\hbar/(m\omega_z\alpha)}$ is a measure for the lateral extension of the electron wave function in the dots. It has been shown in experiments with electrically gated quantum dots in a two-dimensional electron system that the electronic spectrum is well described by a simple harmonic oscillator [25]. In describing the confinement V_v along the inter-dot axis, we have used a (locally harmonic) double well potential of the form

$$V_v = \frac{m\omega_z^2}{8a^2} (z^2 - a^2)^2, \quad (3)$$

which separates into two harmonic wells of frequency ω_z (one for each dot) in the limit $a \gg a_{B\perp}$, where a is half the distance between the dots and $a_{B\perp} = \sqrt{\hbar/m\omega_z}$ is the vertical effective Bohr radius. Although in principle a square-well potential would be a more accurate description of the real potential than the harmonic double well, we believe there is no qualitative difference between the results presented below obtained with harmonic potential and the corresponding results using square-well potential. Finally, the time-dependent electric field has a DC-AC form, i.e., $F(t) = F_0 + F_1 \sin \omega t$.

III. SPIN-1 REPRESENTATION OF THE HAMILTONIAN

Following Burkard *et al.*[22] we employ the Hund-Mulliken method of molecular orbits to describe the low-lying spectrum of our system. This approach accounts for

double occupancies and is therefore suitable for investigating the questions at issue here. As a starting point for our calculations we consider the problem of an electron in a single quantum dot. The one-particle Hamiltonian by which we describe a single electron in the right (left) dot of the double-dot system is

$$h_{\pm a}^0(\mathbf{r}) = \frac{\mathbf{p}^2}{2m} + \frac{m\omega_z^2}{2} (\alpha^2(x^2 + y^2) + (z \mp a)^2), \quad (4)$$

and has the ground-state solution

$$\varphi_{\pm a}(\mathbf{r}) = \left(\frac{m\omega_z}{\pi\hbar} \right)^{3/4} \sqrt{\alpha} \exp \left(-\frac{m\omega_z}{2\hbar} (\alpha^2(x^2 + y^2)) + (z \mp a)^2 \right), \quad (5)$$

corresponding to ground-state energy $\epsilon_{\pm} = \hbar\omega_z(1 + 2\alpha)/2$. The two local ground states are not orthogonal and their overlap is

$$S = \int d^3r \varphi_{+a}^*(\mathbf{r}) \varphi_{-a}(\mathbf{r}) = \exp(-d^2), \quad (6)$$

where the dimensionless parameter $d = a/a_{B\perp}$ denotes the distance between the two dots. A nonvanishing overlap S implies that the electrons can tunnel between the dots. From these non-orthogonal states, we construct the orthonormalized one-particle wave functions

$$\Phi_{+a}(\mathbf{r}) = \frac{1}{\sqrt{1 - 2Sg - g^2}} (\varphi_{+a} - g\varphi_{-a}), \quad (7a)$$

$$\Phi_{-a}(\mathbf{r}) = \frac{1}{\sqrt{1 - 2Sg - g^2}} (\varphi_{-a} - g\varphi_{+a}), \quad (7b)$$

with $g = (1 - \sqrt{1 - S^2})/S$. For appropriate values of system parameters such as the inter-dot distance, the overlap S becomes exponentially small as given in Eq. (7). In this limit an electron in one of the states Φ_{+a} , Φ_{-a} is predominately localized around $(x, y, \pm a)$. In the following we consider this case and use these states to define the localized single-particle state. Schliemann *et al.* [27] have used these two local states as qubits, which are realized by the spin state of an electron in either orbital Φ_{+a} , or orbital Φ_{-a} .

Using $\Phi_{\pm a}$ we generate six basis functions with respect to which we diagonalize the two-particle Hamiltonian H : The states with double occupation, $\Psi_{\mp a}^d(\mathbf{r}_1, \mathbf{r}_2) = \Phi_{\mp a}(\mathbf{r}_1)\Phi_{\mp a}(\mathbf{r}_2)$ [denoted by $(1, 0, 0, 0)^T$ and $(0, 1, 0, 0)^T$, respectively] and the states with single occupation $\Psi_{\pm}^s(\mathbf{r}_1, \mathbf{r}_2) = [\Phi_{+a}(\mathbf{r}_1)\Phi_{-a}(\mathbf{r}_2) \pm \Phi_{-a}(\mathbf{r}_1)\Phi_{+a}(\mathbf{r}_2)]$ [denoted by $(0, 0, 1, 0)^T$ and $(0, 0, 0, 1)^T$, respectively]. Calculating the matrix elements of the Hamiltonian $H(t)$ in this orthonormal basis we get

$$H(t) = \begin{pmatrix} H_1(t) & 0 \\ 0 & (2\epsilon + U_3)I_{1 \times 1} \end{pmatrix} = (2\epsilon + U_3)I_{1 \times 1} \oplus H_1(t), \quad (8)$$

where $I_{1 \times 1}$ is a 1×1 unit matrix, and H_1 is

$$H_1(t) = \begin{pmatrix} 2\epsilon + U_1 + \mu(t) & \sqrt{2}w & v \\ \sqrt{2}w & 2\epsilon + U_2 & \sqrt{2}w \\ v & \sqrt{2}w & 2\epsilon + U_1 - \mu(t) \end{pmatrix} \quad (9)$$

with the matrix elements given by

$$\epsilon = \langle \Phi_{\pm a} | h(z \mp a) | \Phi_{\pm a} \rangle, U_1 = \langle \Psi_{\pm a}^d | C | \Psi_{\pm a}^d \rangle, \quad (10a)$$

$$U_2 = \langle \Psi_+^s | C | \Psi_+^s \rangle, U_3 = \langle \Psi_-^s | C | \Psi_-^s \rangle, \quad (10b)$$

$$w = \langle \Phi_{\pm a} | h(z \mp a) | \Phi_{\mp a} \rangle + \langle \Psi_+^s | C | \Psi_{\pm a}^d \rangle, v = \langle \Psi_{\pm a}^d | C | \Psi_{\pm a}^d \rangle, \quad (10c)$$

$$\mu(t) = \mu_0 + \mu_1 \sin(\omega t) = \frac{2ea(1-g^2)}{1-2Sg+g^2} (F_0 + F_1 \sin \omega t). \quad (10d)$$

Clearly, U_1 denotes the intra-dot Coulomb interaction, whereas U_2 and U_3 describe the inter-dot Coulomb interaction, without particle transfer. w describes single-particle tunneling induced by dot-dot coupling and Coulomb interaction. $\mu_i = 2eF_i a(1-g^2)/(1-2Sg+g^2)$ ($i = 0, 1$) describes the coupling strength between the electrons and external electric fields.

Obviously the spin-triplet state Ψ_-^s is an eigenstate of the Hamiltonian (8) with the electron number on each quantum dot invariably one and has no response to the presence of the electric fields. This is one important fact involving spin-triplet space. Hence we will focus our attention on the reduced spin-singlet Hamiltonian $H_1(t)$. Furthermore, the matrix element v is the amplitude of simultaneous transfer of two electrons and therefore denotes cotunneling process. Compared to the single-electron tunneling term w , this term can be negligible. Thus the reduced Hamiltonian can be conveniently rewritten in terms of spin-1 operators

$$H_1(t) = (2\epsilon + U_2) - \mu(t)J_z + uJ_z^2 + 2wJ_x, \quad (11)$$

where $u = U_1 - U_2$ is the effective Coulomb interaction, and J_i ($i = x, y, z$) are spin-1 operators defined as

$$J_x = \frac{1}{\sqrt{2}} \begin{pmatrix} 0 & 1 & 0 \\ 1 & 0 & 1 \\ 0 & 1 & 0 \end{pmatrix}, \quad (12a)$$

$$J_y = \frac{i}{\sqrt{2}} \begin{pmatrix} 0 & -1 & 0 \\ 1 & 0 & -1 \\ 0 & 1 & 0 \end{pmatrix}, \quad (12b)$$

and

$$J_z = \begin{pmatrix} 1 & 0 & 0 \\ 0 & 0 & 0 \\ 0 & 0 & -1 \end{pmatrix}. \quad (12c)$$

Therefore, the localized two-particle state Ψ_{-a}^d is equivalent to the eigenstate $|j_z = 1\rangle$ of J_z and Ψ_{+a}^d to the state $|j_z = -1\rangle$, whereas the delocalized state Ψ_+^s is identical to the state $|j_z = 0\rangle$. In the following we will denote Ψ_{-a}^d with $|LL\rangle$, Ψ_{+a}^d with $|RR\rangle$, and Ψ_+^s with $|LR\rangle$.

The first term in Eq. (11) denotes a constant energy shift, and will be neglected in the following discussions. The evolution of any initial state $|\Psi(0)\rangle$ under the action of H_1 in Eq. (11) can be expressed as $|\Psi(t)\rangle = C_1(t)|LL\rangle + C_2(t)|LR\rangle + C_3(t)|RR\rangle$ where the coefficients $C_k(t)$ are determined by the time dependent Schrödinger equation (In the following we set $\hbar = 1$)

$$i \frac{d}{dt} \begin{pmatrix} C_1 \\ C_2 \\ C_3 \end{pmatrix} = \begin{pmatrix} u + \mu(t) & \sqrt{2}w & 0 \\ \sqrt{2}w & 0 & \sqrt{2}w \\ 0 & \sqrt{2}w & u - \mu(t) \end{pmatrix} \begin{pmatrix} C_1 \\ C_2 \\ C_3 \end{pmatrix}, \quad (13)$$

and the chosen initial condition $|\Psi(0)\rangle$. In the absence of external electric fields, the eigenenergies of H_1 can be easily solved as

$$E_1 = \frac{1}{2} \left(u - \sqrt{u^2 + 16w^2} \right), \quad (14a)$$

$$E_2 = u, \quad (14b)$$

$$E_3 = \frac{1}{2} \left(u + \sqrt{u^2 + 16w^2} \right), \quad (14c)$$

and the corresponding eigenstates are given as

$$|\varphi_1^{(S)}\rangle = \frac{1}{X} (|LL\rangle - \frac{E_3}{\sqrt{2}w} |LR\rangle + |RR\rangle), \quad (15a)$$

$$|\varphi_2^{(A)}\rangle = \frac{1}{\sqrt{2}} (|RR\rangle - |LL\rangle), \quad (15b)$$

$$|\varphi_3^{(S)}\rangle = \frac{1}{Y} (|LL\rangle - \frac{a}{\sqrt{2}w} |LR\rangle + |RR\rangle), \quad (15c)$$

where we have defined the normalization constants $X = \sqrt{4w^2 + E_3^2}/\sqrt{2}w$ and $Y = \sqrt{4w^2 + E_1^2}/\sqrt{2}w$. The superscript S (A) on the left sides of Eq. (15) denotes symmetry (antisymmetry) under the spatial reflection. We can see from Eq. (15) that due to strong Coulomb repulsion, the symmetric ground state is dominated by the delocalized state $|LR\rangle$, whereas, the other two eigenstates are nearly degenerate and dominated by the two localized states $|LL\rangle$ and $|RR\rangle$. Note that although $|\varphi_2^{(A)}\rangle$ and $|\varphi_3^{(S)}\rangle$ look like a doublet in a single-electron double-trap

system which consists of a pair of symmetric and anti-symmetric single-particle states, there are fundamental differences for the present two-particle system. In fact, the superposition of the two localized states $|LL\rangle$ and $|RR\rangle$ implies that the spatial wave functions of the two electrons have been entangled, in the usual sense that they are not factorized into single-particle states. To describe the degree of entanglement, we define the maximally entangled Bell state

$$|\Psi_{Bell}\rangle = \frac{1}{\sqrt{2}}(|RR\rangle + e^{i\phi}|LL\rangle), \quad (16)$$

with arbitrary phase angle ϕ . Therefore the probability ρ_{Bell} for finding the maximally entangled Bell state in a coupled quantum dot is given by

$$\rho_{Bell} = \frac{1}{2} |C_3(t) + e^{i\phi}C_1(t)|^2. \quad (17)$$

In the following we will investigate the various energy spectrum and consequent dynamics for a GaAs ($m = 0.067m_e$, $\kappa = 13.1$) system comprising two equal dots with vertical confinement energy $\omega_z = 16\text{meV}$ ($a_B = 36\text{nm}$) and lateral confinement energy $\alpha\omega_z = 8\text{meV}$. The inter-dot distance is chosen to be $a = 20\text{nm}$. The corresponding system parameters are calculated to be $u = 5.6\text{meV}$, and $w = -0.15\text{meV}$, implying $|\varphi_1^{(S)}\rangle \simeq |LR\rangle$, and $|\varphi_3^{(S)}\rangle \simeq (1/\sqrt{2})(|RR\rangle + |LL\rangle)$.

IV. LOCALIZATION PREPARATION FROM DELOCALIZED GROUND STATE

We start the search for localization with the simplest case, a constant electric field $F(t) = F_0$. Before $t = 0$ the system is in the delocalized ground state $|\varphi_1^{(S)}\rangle$, and at $t = 0$ the field F_0 is switched on suddenly. We find that when the value of electric field satisfies the following resonance condition

$$F_0 = u, \quad (18)$$

the initial delocalized ground state may be excited into a localized state with two electrons occupying the same right dot. To elucidate this resonance property, we show in Fig. 2 time evolution of the probabilities $P_{LR}(t) = |C_2(t)|^2$ to find the two electrons in the different dots (solid line), $P_{LL}(t) = |C_1(t)|^2$ to find the two electrons in the left dot (dashed line), and $P_{RR}(t) = |C_3(t)|^2$ to find the electrons in the right dot (dotted line). It shows in Fig. 3 that both $P_{LR}(t)$ and $P_{RR}(t)$ oscillate between 0 and 1 with a definite period, while $P_{LL}(t)$ always negligibly small during time evolution, meaning that a complete resonance takes place between the delocalized state $|LR\rangle$ and localized state $|RR\rangle$. In this case, because the population of the localized state $|LL\rangle$ in the left dot

remains almost zero during time evolution, we can neglect its contribution and describe the dynamics by the reduced Schrödinger equation

$$i\frac{d}{dt} \begin{pmatrix} C_2(t) \\ C_3(t) \end{pmatrix} = \begin{pmatrix} 0 & \sqrt{2}w \\ \sqrt{2}w & 0 \end{pmatrix} \begin{pmatrix} C_2(t) \\ C_3(t) \end{pmatrix}. \quad (19)$$

Thus with the initial state $|\Psi(0)\rangle = |\varphi_1^{(S)}\rangle \simeq |LR\rangle$, we have the evolution of the system as follows

$$C_2(t) = \cos(\sqrt{2}wt), \quad (20a)$$

$$C_3(t) = \exp(i\pi/2) \sin(\sqrt{2}wt). \quad (20b)$$

Clearly our two-state approximation Eq. (20) describes the dynamics very well when compared with the exact numerical result shown in Fig. 2, implying complete Rabi oscillation between the localized state $|RR\rangle$ and delocalized state $|LR\rangle$ with oscillation period $\pi/(\sqrt{2}|w|)$.

Once the two electrons are localized, they can be forced to stay localized permanently by switching the field to another nonzero value [see Fig. 3(a)]. We show this effect in Fig. 3(b). This trivial way of keeping localization in a two-electron double-dot system originates from the fact that, due to the presence of constant electric field, the consequent energy mismatch among the three two-particle states prohibit tunneling from the localized state $|RR\rangle$ to the other states.

Another way to implement localized two-particle state is through adiabatically varying the constant electric field, which induces a series of avoided crossings in the energy spectrum. Consequently, the electron number in the ground state will experience a series of Coulomb stairs. This field-induced adiabatic localization is shown in Fig. 4, where Fig. 4(a) plots the evolution of electron number in the right dot for the ground state as a function of the constant electric field, and Fig. 4(b) plots the corresponding energy spectrum. It reveals in Fig. 4 that on adiabatically increasing the strength of constant electric field, a series of avoided crossings develop in the energy spectrum. Consequently, quantum transition occurs at these avoided crossings, resulting in a series of Coulomb stairs. We notice that adiabatically increasing the electric field to a typical value of 2.8kV/cm enables complete localization of the ground state.

V. ENTANGLEMENT OF TWO ELECTRONS IN THE PRESENCE OF CONSTANT ELECTRIC FIELD

As shown in Fig. 2, a resonant constant electric field can induce a complete oscillation between the delocalized state $|LR\rangle$ and localized state $|RR\rangle$. If the constant electric field is turned off [see Fig. 5(a)] at time when the two electrons are fully localized in the right dot, as shown in Fig. 2(b), the strong Coulomb repulsion will

induce the resonance between the localized states $|RR\rangle$ and $|LL\rangle$ during subsequent evolution, whereas the delocalized state $|LR\rangle$ is inhibited to be occupied. This dark property of the delocalized state is shown in Fig. 5(b). It reveals in Fig. 5(b) that the value of P_{LR} is almost zero during time evolution, suggesting that the two electrons are never separated into different dots. While cycling from one dot to the other, the two electrons are always correlated and entangled, and very likely to be found in the same dot.

The entanglement between the two electrons illustrated in Fig. 5(b) can be well described by a two-state approximation. Because the population of the delocalized state $|LR\rangle$ remains very small after time $t_0 = \pi/(2\sqrt{2}|w|)$ shown in Fig. 4(b), we can approximate $C_2(t)$ ($t > t_0$) in Eq. (13) to first order of w/u

$$C_2(t) = \frac{-\sqrt{2}w}{u} \exp(-iut)[C_1(t) + C_3(t)]. \quad (21)$$

By introducing $C_2(t)$ from Eq. (21) in the Schrödinger equation we reduce the system to an effective two-level system. The reduced equation has the form

$$i\frac{d}{dt} \begin{pmatrix} C_1(t) \\ C_3(t) \end{pmatrix} = \begin{pmatrix} u & -2w^2/u \\ -2w^2/u & u \end{pmatrix} \begin{pmatrix} C_1(t) \\ C_3(t) \end{pmatrix}. \quad (22)$$

Thus with the initial state $|\Psi(t_0)\rangle = -i|RR\rangle$ [see Eq. (20)], we have the following time evolution of the system

$$C_1(t) = \exp(-iut) \sin(2w^2t/u), \quad (23a)$$

$$C_3(t) = -i \exp(-iut) \cos(2w^2t/u). \quad (23b)$$

Substituting Eq. (23) into Eq. (17) we have the probability to find the Bell state $(|RR\rangle + e^{i\phi}|LL\rangle)/\sqrt{2}$ at time t

$$\rho_{Bell}(t) = \frac{1}{2}[1 + \sin(\omega_r t) \cos(\phi + \pi/2)], \quad (24)$$

where $\omega_r = 4w^2/\kappa$. In particular we can see from Eq. (23) that the system's quantum state at time

$$\tau = \pi u/8w^2 + t_0, \quad (25)$$

corresponds to a $\phi = -\pi/2$ maximally entangled Bell state $(|RR\rangle - i|LL\rangle)/\sqrt{2}$.

We present in Fig. 5(c) (solid line) the probability for finding the maximally entangled Bell state ($\phi = -\pi/2$) as a function of time. The system parameters are the same as that used in Fig. 5(b). Clearly our two-state approximation [Eq. (24)] describes the system's evolution very well when compared with the exact numerical solution shown in Fig. 5(c), implying that the system's quantum state at time τ corresponds to a maximally entangled Bell state ($\phi = -\pi/2$). However, the degree of entanglement degrades after time τ , a consequence of the fact

that the state at time τ is not an eigenstate of the field-free Hamiltonian. So a single pulse of constant electric field can not preserve the entanglement in our system. Note that no maximally entangled Bell-state generation is possible if the effective Coulomb interaction κ , along with the electric field, is turned off, as shown in Fig. 5(c) (dotted line). This implies essential role of the nonlinear Coulomb interaction in forming the entanglement between the electrons.

VI. ENTANGLEMENT OF TWO ELECTRONS IN THE PRESENCE OF OSCILLATORY ELECTRIC FIELD

We turn now to discussion of the entanglement in the presence of a sinusoidal field of the form $F(t) = F_1 \sin \omega t$. Figure 6 illustrates the spectral features by plotting the Floquet quasienergies as a function of driving frequency ω . The amplitude value of the field is chosen to be $F_1 = 1.5\text{kV/cm}$. It shows in Fig. 6 that on adiabatically increasing the value of ω , the quasienergies ε_1 and ε_3 approach each other. Especially when the value of driving frequency satisfies

$$\omega = u, \quad (26)$$

an avoided crossing occurs in the quasienergy spectrum.

To elucidate the effect of the avoided crossing displayed in Fig. 6 on the quantum mechanical behavior of the system, we examine the dynamics of the system starting with unperturbed ground state, i.e., $|\Psi(0)\rangle = |\varphi_1^{(S)}\rangle$. Figure 7(a) shows time evolution of the probabilities $P_{LR}(t)$ (solid line), $P_{LL}(t)$ (dashed line), and $P_{RR}(t)$ (dotted line). With the system parameters corresponding to the avoided crossing shown in Fig. 6. It reveals in Fig. 7(a) that the two electrons oscillate between the delocalized state $|LR\rangle$ and two localized states $|LL\rangle$ and $|RR\rangle$. The occupations of two localized states are always the same and the oscillations are in-phase. The maximum values of $P_{LL}(t)$ and $P_{RR}(t)$ are 0.5, which corresponds to zero occupation of state $|LR\rangle$. Figure 7(b) shows the probability ρ_{Bell} to find the maximally entangled Bell state with $\phi = \pi$. We can see from Fig. 7(b) that the degree of entanglement varies with time. In particular when the occupation of delocalized state $|LR\rangle$ is zero, the two electrons are maximally entangled with $\rho_{Bell} = 1$.

Once the two electrons are in the maximally entangled Bell state, they can remain maximally entangled by suddenly turning off the oscillatory electric field [see Fig. 8(a)]. We show this effect in Figs. 8(b)-(c) where Fig. 8(b) plots time evolution of the occupations of three two-particle states and Fig. 8(c) the probability to find the maximally entangled Bell state with $\phi = \pi$ (solid line). It shows in Fig. 8(b) that a pulse of oscillatory electric field induces the two electrons to stay on the same dot, while each of them occupies either of the dots with the same probability. It reveals in Fig. 8(c) (solid line) that the

two electrons remain maximally entangled during time evolution after the oscillatory field is turned off. This is different from what is shown in Fig. 5(c) where the degree of entanglement varies with time. Therefore, by a pulse of oscillatory electric field with frequency satisfying the resonant condition Eq. (26), the maximally entangled Bell state can be created and maintained. Loss and Di-vincenzo studied entanglement in double quantum dots involving the spin degree of freedom [21]. Here we have identified a complementary method that creates and preserves entanglement between the spatial wave functions of two electrons in a coupled quantum dot.

The generation of maximally entangled Bell state shown in Fig. 8 can be well described by a two-state approximation. Taking into account symmetric properties of the three unperturbed eigenstates of the system, the dynamics is determined by the one-photon transition between the ground state $|\varphi_1^{(S)}\rangle$ and the first excited two-particle state $|\varphi_2^{(A)}\rangle$, whereas the transition from $|\varphi_1^{(S)}\rangle$ to $|\varphi_3^{(S)}\rangle$ is prohibited due to their identical symmetry. In this case, we can approximate the Hamiltonian $H_1(t)$ in a Hilbert space spanned by the states $|\varphi_1^{(S)}\rangle$ and $|\varphi_2^{(A)}\rangle$

$$H_1(t) = \begin{pmatrix} E_1 & -\sqrt{2}\mu_1(t)/X \\ -\sqrt{2}\mu_1(t)/X & E_2 \end{pmatrix}. \quad (27)$$

In the interaction representation and after applying the rotating-wave approximation (RWA) the Schrödinger Equation takes the form

$$i\frac{d}{dt} \begin{pmatrix} d_1 \\ d_2 \end{pmatrix} = \begin{pmatrix} 0 & -\Omega_r \\ -\Omega_r & \Delta \end{pmatrix}, \quad (28)$$

where d_1 and d_2 are the probability amplitudes of the bare states $|\varphi_1^{(S)}\rangle$ and $|\varphi_2^{(A)}\rangle$, $\Omega_r = V_1/\sqrt{2}X$ is Rabi frequency, and $\Delta = E_2 - E_1 - \omega$ is the detuning of the driving frequency ω from the transition frequency. In the case of one-photon resonance $E_2 - E_1 = \omega$, we obtain the time evolution of initial ground state ($d_1(0) = 1$, $d_2(0) = 0$) as follows

$$d_1 = \cos \Omega_r t, \quad (29a)$$

$$d_2 = i \sin \Omega_r t. \quad (29b)$$

Thus the system oscillates between the ground state wherein two electrons are highly delocalized and the first excited state wherein the two electrons are highly entangled. Substituting Eq. (29) into Eq. (17), and in the weak coupling limit $w \ll u$, we obtain the expression for the probability to find the maximally entangled Bell state

$$\rho_{Bell}(t) = \frac{1}{2}(1 - \cos \phi) \sin^2(w\mu_1 t/u), \quad (30)$$

where we have approximated Rabi frequency Ω_r with $w\mu_1/u$. In particular we can see from Eq. (29) that the quantum state of the system at time

$$\tau = \pi u/(2w\mu_1), \quad (31)$$

corresponds to a $\phi = \pi$ maximally entangled Bell state $(|RR\rangle - |LL\rangle)/\sqrt{2}$.

The result of Eq. (30) is shown in Fig. 8(c) (dotted line). Clearly, in comparison with the exact numerical solution, our two-state approximation describes the system evolution very well, suggesting that the quantum state of system at time $\tau = \pi u/(2w\mu_1)$ corresponds to a maximally entangled Bell state of the desired form with $\phi = \pi$. Therefore we arrive at the conclusion that a selective pulse of oscillatory electric field with duration $\tau = \pi u/(2w\mu_1)$ can be used to create and maintain a maximally entangled Bell state ($\phi = \pi$) in the system of two electrons in a coupled quantum dot.

We notice from Eq. (31) that Bell-state generation time is significantly shortened by increasing the amplitude of the oscillatory electric field. This is important because shorter Bell-state generation time is fundamental to the experimental observation of such maximally entangled state, which is impeded by inevitable decoherence occurred in the realistic double quantum dot system. The decoherence is the most problematic issue pertaining to most quantum computing processing. In the present entangled state proposal, the decohering time depends partly on the fluctuation of the single particle energy caused by the modification of the confining potential due to phononic excitations. There is also a quantum electrodynamic contribution because of coupling to the vacuum modes. In addition, impurity scattering and phonon emission also have contributions to the decoherence. However, in principle, their effects can be minimized by more precise fabrication technology and by cooling the system.

VII. DYNAMICAL LOCALIZATION OF TWO INTERACTING ELECTRONS

In section IV we have shown that a trivial way of maintaining localization is to suddenly shift the constant field to another value once the electrons are in the localized state $|RR\rangle$. In this section we study the possibility of remaining the localization with the oscillatory electric field $F(t) = F_1 \sin \omega t$ [22]. Because the localized state $|RR\rangle$ may be always produced from the ground state as described above, we therefore suppose in the following discussions that the system starts with the localized state $|RR\rangle$.

In the presence of time-dependent electric field, the evolution of the system can not be solved in a closed form because $[H_1(t_1), H_1(t_2)] \neq 0$. However, time periodicity of the Hamiltonian (11) enables us to describe the dynamics within the Floquet formalism. We numerically integrate the motion of equation for time evolution operator

$$i\frac{\partial}{\partial t} U(t, 0) = H_1(t)U(t, 0), \quad (32)$$

and diagonalize $U(2\pi/\omega, 0)$ to obtain the quasienergies $\{\varepsilon_{\alpha,l}\}$ and Floquet states $\{|u_{\alpha,l}(0)\rangle\}$ at time $t = 0$. Here the quasienergies $\varepsilon_{\alpha,l}$ are confined to the first Brillouin zone and, at $F_1 = 0$, connected to $E_\alpha + l\omega$. The index l counts ‘how many photons’ have to be subtracted from the unperturbed energy level E_α in order to arrive in the first Brillouin zone. The Floquet state $|u_{\alpha,l}(t)\rangle$ can be obtained from the eigenvalue equation

$$(H_1(t) - i\frac{\partial}{\partial t}) |u_{\alpha,l}(t)\rangle = \varepsilon_{\alpha,l} |u_{\alpha,l}(t)\rangle, \quad (33)$$

where $\alpha = 1, 2, 3$. Note that the Hamiltonian (11) remains invariant under the combined spatial reflection and time translation $t \rightarrow t + \pi/\omega$. An immediate consequence of this dynamical symmetry is that each Floquet state is either odd or even [28,29]. When the driving amplitude is switched off adiabatically, $F_1 \rightarrow 0$, the Floquet states are connected with the stationary eigenstates in Eq. (15) as follows [1]

$$|u_{\alpha,l}(t)\rangle \rightarrow |u_{\alpha,l}^0(t)\rangle = \varphi_\alpha \exp(il\omega t). \quad (34)$$

Thus we can easily determine the dynamical parity of the Floquet state $|u_{\alpha,l}(t)\rangle$.

We present in Figs. 9(a)-(b) the quasienergies versus the amplitude F_1 , where the values of driving frequency ω are respectively chosen to satisfy $u = 3.1\omega$ and $u = 2\omega$, respectively. In Fig. 9(a) we see that the quasienergies $\varepsilon_{2,-3}$ and $\varepsilon_{3,-3}$ with different parity form an exact crossing at $F_1 = 1.05\text{kV/cm}$. When $F_1 \rightarrow 0$, all three quasienergies arrive at the unperturbed cases by $\varepsilon_{1,0}^0 = E_1$, $\varepsilon_{2,-2}^0 = E_2 - 3\omega$, $\varepsilon_{3,-2}^0 = E_3 - 3\omega$. For $2l\omega \rightarrow E_2 - E_1$, $\varepsilon_{1,0}$ and $\varepsilon_{3,-2l}$, belonging to different parity, are also allowed to cross, as shown in Fig. 9(b) where the value of index is $l = 1$. In the exact same way, when $(2l+1)\omega \rightarrow E_3 - E_1$ two quasienergies $\varepsilon_{1,0}$ and $\varepsilon_{3,-(2l+1)}$ can develop into the crossing for special value of the amplitude F_1 (not shown here).

To elucidate the effect of the exact crossing on the quantum mechanic behavior of the system we present in Fig. 10(a) the time evolution of $P_{RR}(t)$ with the system parameters corresponding to the first crossing between $\varepsilon_{2,-3}$ and $\varepsilon_{3,-3}$ shown in Fig. 9(a). For comparison we also plot $P_{RR}(t)$ in Fig. 10(b) for the value of amplitude $F_1 = 0.5\text{kV/cm}$. In Fig. 10(a) we can see that during time development the probability $P_{RR}(t)$ remains near 1 as if the two electrons were frozen in the right dot. Thus at the exact crossing of $\varepsilon_{2,-3}$ and $\varepsilon_{3,-3}$ the dynamical localization builds up although the strong Coulomb repulsion between the two electrons prevents the system behaving so. Note that the value of u used in Fig. 10(a) corresponds to the unperturbed energies $E_1 = -0.016\text{meV}$, $E_2 = 5.6\text{meV}$, and $E_3 = 5.616\text{meV}$. Because E_1 is much lower than E_2 and E_3 , the unperturbed eigenstates φ_2^A and φ_3^S , both of which have a very small component of the delocalized two-particle state $|LR\rangle$, become comparable to a doublet in a symmetrical double-dot system. So it is expected that at the

crossing of the quasienergies $\varepsilon_{2,-3}$ and $\varepsilon_{3,-3}$ the initial localized state can be approximated by a superposition of degenerate Floquet states $|u_{2,-3}(0)\rangle$ and $|u_{3,-3}(0)\rangle$, which remains localized in perpetuity. This looks like the case of a single-electron, two-level system consisting of the lowest symmetric and antisymmetric states of the double-trap potential, where perfect localization can be achieved at the exact crossing between the two Floquet quasienergies. It is numerically found that even if the Coulomb interaction u is strong enough, the dynamical localization can still occur so long as the quasienergies $\varepsilon_{2,m}$ and $\varepsilon_{3,m}$ cross each other. Moreover, the value of the system parameter $2\mu_1/\omega$ corresponding to the first crossing is about 2.4, which is a root of the zero-order Bessel function, suggesting that in this situation the dynamical localization can be approximated by the driven two-level model. If the system parameters deviate from the level crossing, then the dynamical localization ceases to exist and P_{RR} oscillates between 0 and 1 in the time development, as shown in Fig. 10(b).

More surprisingly, we notice that compared with non-interacting ($u = 0$) case, the presence of Coulomb repulsion enhances the degree of localization to a larger extent. To illustrate this feature we present in Fig. 10(c) time evolution of P_{RR} with the parameters corresponding to the first exact crossing of the quasienergies in the absence of Coulomb interaction. It shows in Fig. 10(c) that although dynamical localization maintains during time development, the degree of localization is much lower than that shown in Fig. 10(a), suggesting Coulomb-enhanced localization. From Eq. (15) we know that due to strong Coulomb interaction, the initial localized state $|RR\rangle$ can be approximated by a superposition of two eigenstates $|\varphi_2^{(A)}\rangle$ and $|\varphi_3^{(S)}\rangle$ as $|RR\rangle \simeq (1/\sqrt{2})(|\varphi_2^{(A)}\rangle + |\varphi_3^{(S)}\rangle)$. Thus from what we have learned in single-particle double-trap system, it is not difficult to understand why the localization can be dynamically remained at the exact crossing of two Floquet states developed from $|\varphi_2^{(A)}\rangle$ and $|\varphi_3^{(S)}\rangle$. Similarly, in the absence of Coulomb interaction, the initial localized state $|RR\rangle$ can be approximated by a superposition of all three eigenstates as $|RR\rangle = (1/\sqrt{2})(|\varphi_1^{(S)}\rangle + |\varphi_2^{(A)}\rangle + |\varphi_3^{(S)}\rangle)$, suggesting dynamical localization at the crossing among three quasienergies. However, the fundamental difference lies in the fact that when the strong interaction is present, the tunneling coupling is $\langle LL|H_1|RR\rangle = E_3 - E_2 \simeq 4w^2/u$. In the absence of Coulomb interaction, whereas, the tunneling coupling is $\langle LL|H_1|RR\rangle = (1/2)(E_1 + E_3) - E_2 = 2w$. Thus we can see that the coupling between the two localized states greatly decreases in the presence of strong Coulomb interaction, which leads to fundamental increase of localization degree.

We turn to study the dynamics of the system at the crossing of the quasienergies $\varepsilon_{1,0}$ and $\varepsilon_{2,-2}$ in Fig. 9(b), using the same initial state condition. The result is shown in Fig. 10(d). In contrary to that shown in Fig. 10(a), it shows in Fig. 10(d) that at the level crossing of $\varepsilon_{1,0}$

and $\varepsilon_{2,-2}$ dynamical localization does not happen and $P_{RR}(t)$ oscillates between 0 and 1. Note that the level crossing of $\varepsilon_{1,0}$ and $\varepsilon_{2,-2}$ induces strong participation of the Floquet state $|u_{1,0}(t)\rangle$ during the time evolution of the system, and the most component in $|u_{1,0}(t)\rangle$ is the delocalized two-particle state $|LR\rangle$. Therefore the strong mixture of the Floquet state $|u_{1,0}(t)\rangle$ in the evolution of the system will lead to complete destruction of the dynamical localization, as shown in Fig. 10(d).

In the above discussions we have ignored higher-lying single-particle states; this requires that the frequency of the external field is much lower than single-particle level spacing. In the presence of decoherence due to environmental dissipation, long dephasing time should be required. A detailed analysis of the effect of a decohering environment will be given elsewhere.

VIII. CONCLUSIONS

In conclusion we have shown how dynamical localization and entanglement of two interacting electrons in a double quantum dot system can be accessed by external electric fields. We have found that (i) The presence of a constant electric field may induce the complete Rabi oscillation between the delocalized state $|LR\rangle$ and localized state $|RR\rangle$. Thus Starting from the delocalized ground state, we can prepare a fully localized state. The localization can be maintained by switching the field to another nonzero value. (ii) The two electrons oscillate between the delocalized state and two localized states in the presence of a resonant oscillatory field. With the oscillatory field turned off at time when the probabilities for finding the electrons in the left and right dot are identically 0.5, the two electrons remain maximally entangled in the subsequent time evolution. Thus a selective pulse of oscillatory field can be used to implement maximally entangled Bell states in a two-electron two-dot system. (iii) Although the Coulomb repulsion is very strong, the two initially localized electrons can stay localized during time evolution. It is also shown that compared to non-interacting case, the Coulomb interaction enhances the degree of localization to a larger extent. We expect the present results are useful in exploiting the coherent control of electrons in quantum dot systems.

ACKNOWLEDGMENTS

This work was supported partly by the National Natural Science Foundations of China under Grant No. .

[1] M. Grifoni and P. Hänggi, Phys. Rep. **304**, 229 (1998).
[2] F. Grossmann, T. Dittrich, P. Jung, and P. Hänggi, Phys. Rev. Lett. **67**, 516 (1991).

[3] R. Bavli and H. Metiu, Phys. Rev. Lett. **69**, 1986 (1992).
[4] J. M. Gomez Llorente and J. Plata, Phys. Rev. A **45**, R6958 (1992).
[5] F. Grossmann and P. Hänggi, Europhys. Lett. **18**, 571 (1992).
[6] M. Holthous and D. Hone, Phys. Rev. B **47**, 6499 (1993).
[7] R.I. Cukier and M. Morillo, Chem. Phys. **183**, 375 (1994).
[8] T. Zuo, S. Chekowski, and A.D. Bandrauk, Phys. Rev. A **49**, 3943 (1994).
[9] H. Pu, S. Raghavan, and N. P. Bigelow, Phys. Rev. A **61**, 023602 (2000).
[10] P. Zhang, A.Z. Zhang, S.Q. Duan, and X.-G. Zhao, Phys. Lett. A **287**, 105 (2001).
[11] P. Zhang, Q.-K. Xue, X.-G. Zhao, and X.C. Xie, Phys. Rev. A **66**, 022117 (2002).
[12] P.I. Tamborenea and H. Metiu, Europhys. Lett. **53**, 776 (2001).
[13] A. Steane, Rep. Prog. Phys. **61**, 117 (1998).
[14] Q.A. Turchette, C.S. Wood, B.E. King, C.J. Myatt, D. Leibfried, W.M. Itano, C. Monroe, and D.J. Wineland, Phys. Rev. Lett. **81**, 3631 (1998).
[15] E. Hagley, X. Maitre, G. Nogues, C. Wunderlich, M. Brune, J.-M. Raimond, and S. Haroche, Phys. Rev. Lett. **79**, 1 (1997).
[16] A. Rauschenbeutel, G. Nogues, S. Osnaghi, P. Bertet, M. Brune, J.-M. Raimond, and S. Haroche, Science **288**, 2024 (2000).
[17] C.A. Sackett, D. Kielpinski, B.E. King, C. Langer, V. Meyer, C.J. Myatt, M. Rowe, Q.A. Turchette, W.M. Itano, D.J. Wineland, and C. Monroe, Nature **404**, 256 (2000).
[18] F. R. Waugh, M. J. Berry, D. J. Mar, R. M. Westvelt, K. L. Campman, and A. C. Gossard, Phys. Rev. Lett. **75**, 705 (1995); C. Livermore, C. H. Crouch, R. M. Westvelt, K. L. Campman, and A. C. Gossard, Science **274**, 1332 (1996); R. H. Blick, D. Pfannkuche, R. J. Haug, K. v. Klitzing, and K. Eberl, Phys. Rev. Lett. **80**, 4032 (1998); R. H. Blick, D. W. vander Weide, R. J. Haug, and K. Eberl, *ibid.* **81**, 689 (1998). See also references in these publications.
[19] For recent articles on double quantum dots with few electrons see: Y. Tokura, D.G. Austing, and S. Tarucha, J. Phys.: Condens. Matter **11**, 6023 (1999); B. Partoens, A. Matulis, and F.M. Peeters, Phys. Rev. B **59**, 1617 (1999); D.G. Austing, T. Honda, K. Muraki, Y. Tokura, and S. Tarucha, Physica B **249**, 206 (1998); and references therein.
[20] B.E. Kane, Nature **393**, 133 (1998).
[21] D. Loss, and D.P. DiVincenzo, Phys. Rev. A **57**, 120 (1998).
[22] P. Zhang and X.-G. Zhao, Phys. Lett. A **271**, 419 (2000).
[23] A. Imamoglu, D.D. Awschalom, G. Burkard, D.P. DiVincenzo, D. Loss, M. Sherwin, and A. Small, Phys. Rev. Lett. **83**, 4204 (1999).
[24] L. Quiroga and N.F. Johnson, Phys. Rev. Lett. **83**, 2270 (1999).
[25] L. Jacak, P. Hawrylak, and A. Wójs, *Quantum dots* (Springer, Berlin, 1997).
[26] G. Burcard, G. Seelig, and D. Loss, preprint (cond-mat/9910105).
[27] J. Schliemann, D. Loss, and A.H. MacDonald, preprint (cond-mat/0009083).

[28] A. Peres, Phys. Rev. Lett. **67**, 158 (1991).
 [29] J. Y. Shin and H. W. Lee, Phys. Rev. E **53**, 3096 (1996).

Figure captions

Fig. 1 Sketch of two interacting electrons in a coupled quantum dot driven by electric fields.

Fig. 2. Time evolution of the probabilities P_{LR} (solid line), P_{LL} (dashed line), and P_{RR} (dotted line) for the value of the strength of constant electric field satisfying resonant condition $\mu_0 = u$.

Fig. 3. (a) Electric field that imposes on the double quantum dot system; (b) Time evolution of the probabilities P_{LR} (solid line) and P_{RR} (dotted line) under the influence of the electric field shown in (a). The other system parameters are the same as that used in Fig. 2.

Fig. 4. (a) Electron number distribution of right dot in the ground state as a function of the strength of constant electric field; (b) Energy spectrum of the driven two-electron system as a function of the strength of a constant electric field.

Fig. 5. (a) Electric field that imposes on the double quantum dot system; (b) Time evolution of the probabilities P_{LR} (solid line) and P_{RR} (dotted line) under the influence of the electric field shown in (a); (c) Time evolution of the probability ρ_{Bell} for finding the maximally entangled Bell state ($\phi = -\pi/2$) in the presence of the Coulomb interaction (solid line) and in the absence of the Coulomb interaction (dotted line).

Fig. 6. Quasienergy spectrum of the driven two-electron system as a function of the frequency of oscillatory electric field.

Fig. 7. (a) Time evolution of the probabilities P_{LR} (solid line), P_{LL} (dashed line), and P_{RR} (dotted line) for the value of the frequency of oscillatory electric field $\omega = u$; (b) Time evolution of the probability ρ_{Bell} for finding the maximally entangled Bell state ($\phi = \pi$). The system parameters are the same as that used in (a).

Fig. 8. (a) Electric field that imposes on the double quantum dot system; (b) Time evolution of the probabilities P_{LR} (solid line), P_{LL} (dashed line), and P_{RR} (dotted line) under the influence of the electric field shown in (a); (c) Exact numerical (solid line) and approximate analytic (dotted) results of time evolution of the probability ρ_{Bell} for finding the maximally entangled Bell state ($\phi = \pi$) in a coupled quantum dot. The other system parameters are the same as that used in Fig. 7.

Fig. 9. Floquet spectrum of the driven two-electron system as a function of the strength of oscillatory electric field for the value of the effective Coulomb interaction (a) $u = 3.1\omega$; (b) $u = 2\omega$.

Fig. 10. Time evolution of the probability $P_{RR}(t)$ for four different kinds system parameter values (a) $u = 3.1\omega$ and $F_1 = 1.05\text{kV/cm}$, corresponding to the exact level crossing shown in Fig. 9(a); (b) $u = 3.1\omega$ and $F_1 = 0.5\text{kV/cm}$, for comparison with the case shown in (a); (c) $u = 0$, $\omega = 1.81\text{meV}$, and $F_1 = 2\text{kV/cm}$, corresponding to the exact level crossing in the absence of Coulomb interaction; (d) $u = 2\omega$ and $F_1 = 0.52\text{kV/cm}$,

corresponding to the exact level crossing shown in Fig. 9(b).

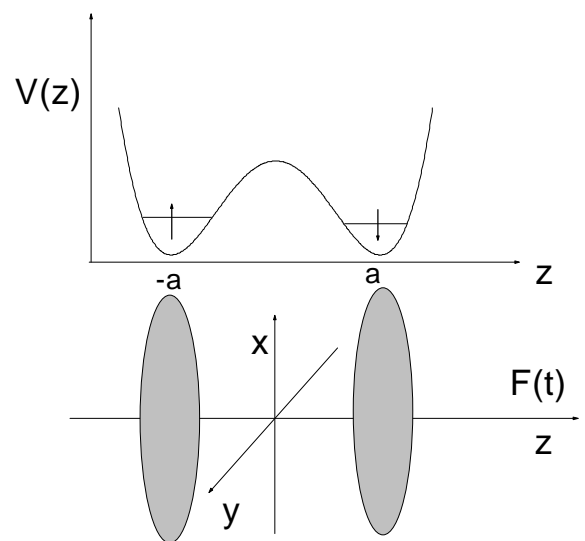


Fig. 1

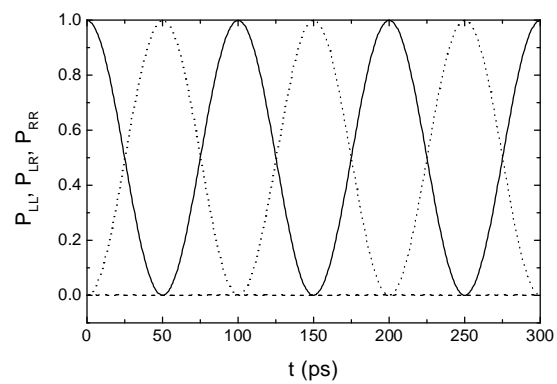


Fig. 2

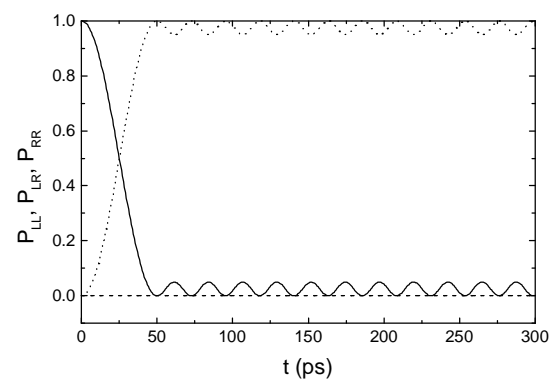


Fig. 3

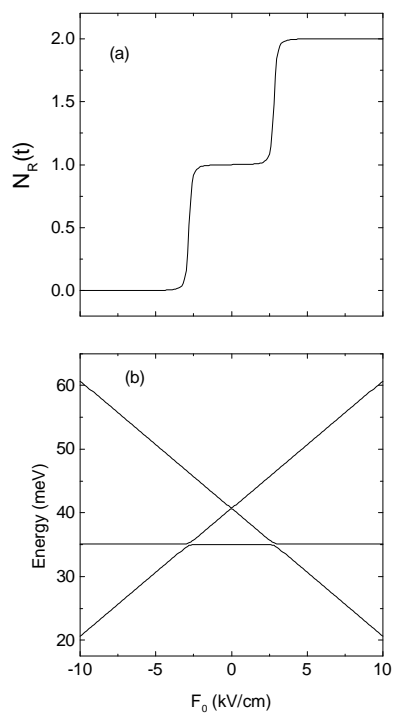


Fig. 4

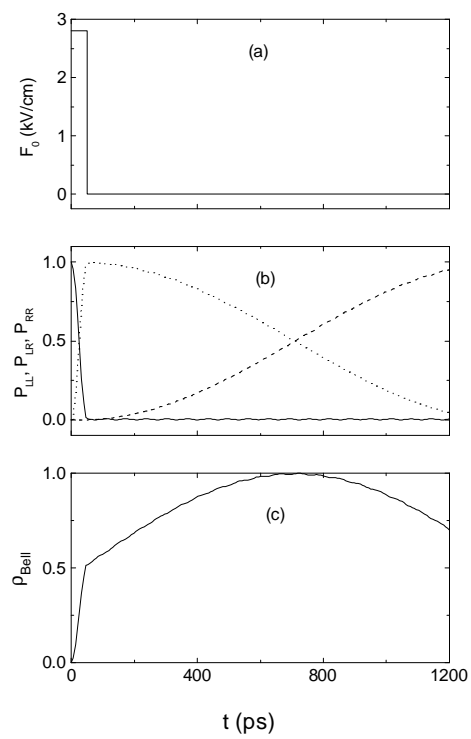


Fig. 5

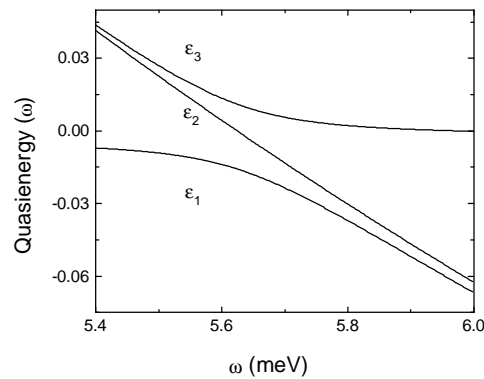


Fig. 6

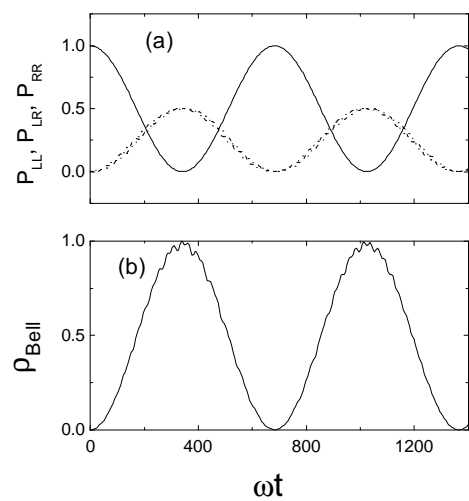


Fig. 7

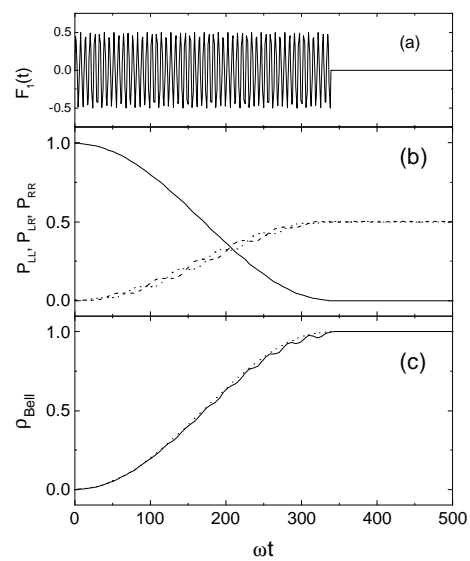


Fig. 8

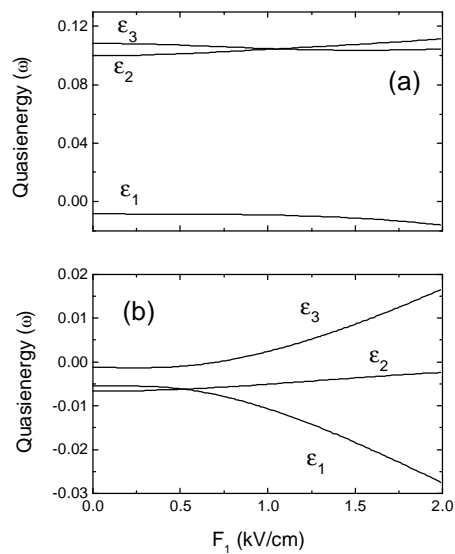


Fig. 9

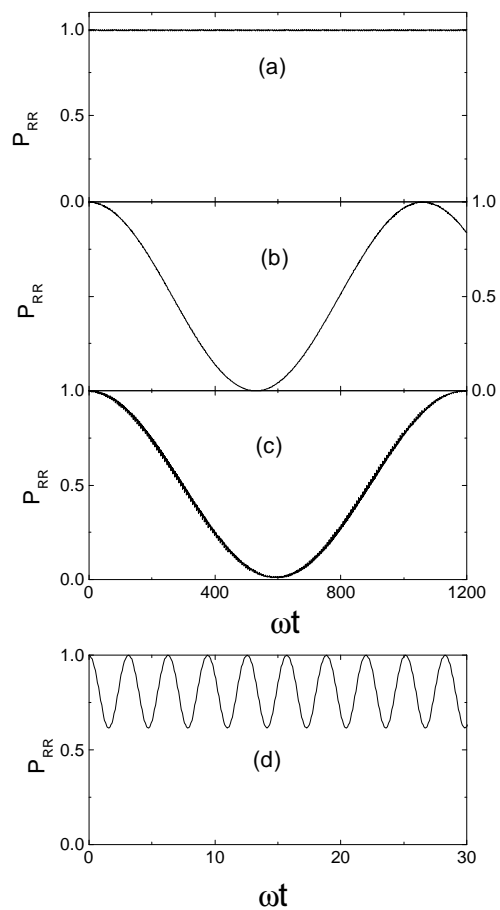


Fig. 10